

Topological strata of weighted complex networks

Giovanni Petri^{1,*}, Martina Scolamiero^{1,2}, Irene Donato^{1,3} Francesco Vaccarino^{1,3}

1 ISI Foundation, Via Alassio 11/c, 10126 Torino - Italy

2 Dipartimento di Ingegneria Gestionale e della Produzione, Politecnico di Torino, C.so Duca degli Abruzzi n.24, Torino, 10129, Italy

3 Dipartimento di Scienze Matematiche, Politecnico di Torino, C.so Duca degli Abruzzi n.24, Torino, 10129, Italy

* E-mail: giovanni.petri@isi.it

Abstract

The statistical mechanical approach to complex networks is the dominant paradigm in describing natural and societal complex systems. The study of network properties, and their implications on dynamical processes, mostly focus on locally defined quantities of nodes and edges, such as node degrees, edge weights and –more recently– correlations between neighboring nodes. However, statistical methods quickly become cumbersome when dealing with many-body properties and do not capture the precise mesoscopic structure of complex networks.

Here we introduce a novel method, based on persistent homology, to detect particular non-local structures, akin to *weighted holes* within the link-weight network fabric, which are invisible to existing methods. Their properties divide weighted networks in two broad classes: one is characterized by small hierarchically nested holes, while the second displays larger and longer living inhomogeneities. These classes cannot be reduced to known local or quasilocal network properties, because of the intrinsic non-locality of homological properties, and thus yield a new classification built on high order coordination patterns. Our results show that topology can provide novel insights relevant for many-body interactions in social and spatial networks. Moreover, this new method creates the first bridge between network theory and algebraic topology, which will allow to import the toolset of algebraic methods to complex systems.

1 Introduction

Complex networks have become one of the prominent tools in the study of social, technological and biological systems [1, 2, 3]. In particular, weighted networks have been largely used to convey not only the presence but also the intensity of relations between nodes in a network. Real-world networks display however intricate patterns of redundant links with edge weights and node degrees usually ranging over various orders of magnitudes [4, 5]. This makes very hard to extract the significant network structure from the background [6, 7, 8, 9], especially in the case of very dense networks [10, 11]. Alongside topological filtering methods [13, 12], the typical approach to this problem is to choose a suitable threshold for the edge weights, e.g. global [10] or local [14], and study the reduced graph composed by only the edges of weight larger (smaller) than the threshold parameter. In any case, some properties of the original graph are inevitably lost under such transformation.

To avoid this pitfall, we propose to consider the set of all filtered networks, ordered by the descending thresholding weight parameter, in the spirit of *persistent homology* [15, 16, 17].

This set, which we call *graph filtration*, combines link weights and connectivity structure over all weight scales. The graph filtration proceeds on the network Ω following these steps:

- Rank the weights of links from ω_{max} to ω_{min} : the discrete parameter ϵ_t scans the sequence.
- At each step t of the decreasing edge ranking we consider the thresholded graph $G(\omega_{ij}, \epsilon_t)$, i.e. the subgraph of Ω with links of weight larger than ϵ_t .

Figure 1a provides a schematic illustration of the rank filtration. This approach preserves the complete topological and weight information, allowing us to focus on special mesoscopic structures: *weighted network holes*, that relate the network’s weight-degree structure to its homological backbone.

A weighted network hole of weight ω is a loop composed by n nodes $i_0, i_1, i_2, \dots, i_{n-1}$, where all cyclic edges (i_l, i_{l+1}) (with $i_0 \equiv i_n$) have weights $\geq \omega$, while all the other possible edges crossing the loop are strictly weaker than ω . We focus on this special class of subgraphs, because formally such weighted holes are generators of the first homology group, H_1 , of the clique complex of the graph thresholded by weight ω (see Materials and Methods). The aim of this paper is to characterize the evolution of these generators along the network filtration. As we swipe the network from the largest to the smallest weights, network holes appear and potentially close.

By unearthing their properties, we obtain the main contribution of this paper: the statistical features of weighted network holes yield a classification of real-world networks in two classes, depending on the compatibility or lack thereof with null models generated by graph randomisations. Furthermore, this classification is defined by mesoscopic homological structures that cannot be reconduced to local properties alone.

The method used for the classification itself, which we call *weighted clique rank homology*, is the second novel main contribution of this paper. It allows to recover complete and accurate long-range information from noisy redundant network data, by building on persistent homology [16], a recent theory developed in computational topology [17], which we extend to the case of networks.

Each weighted hole g is characterized by three quantities: its birth index β_g , its persistence p_g and its length λ_g . After ranking links in a descending order according to their weights, the birth index of a hole is the rank t of its weight ω . As we proceed adding links to the filtration in ranking order, it is possible that a link with rank $t' > t$ will appear and cross the hole. We call this closure of the weighted hole, or *death* δ_g . The persistence p_g is the interval between the birth and death of g , $p_g = \delta_g - \beta_g = t' - t$. Finally, the length λ_g is the number of links composing g .

Similarly to stratigraphy, each step of the filtration is a topological stratum of the network, where the edge weight rank plays the role of depth. Intuitively, g can then be thought as an underground cavity, hidden in the link-weight fabric of the network, and β_g , p_g and λ_g as its maximal depth, vertical size and girth respectively.

2 Results

2.1 Homological network classes

We applied this analysis to various social, infrastructural and biological networks (see SI for a detailed list). In order to compare datasets, indices are normalized by the corresponding filtration length (maximal rank) T , so that all β_g , δ_g , and thus p_g , vary in the unit interval. In addition, we compared each dataset with two randomized versions, obtained by weight reshuffling and edge-swapping respectively. While both randomisations preserve the weight and degree sequences, the first one redistributes the edge weights and is meant to destroy weight correlations, while preserving the linking patterns and thus the degree assortativity. The second instead randomizes the network through double-edge swaps, destroying both weight and degree correlations [22]. We stress that, as the degree and weight sequences are preserved in the randomisations, they cannot account for the differences in the observed homology.

The statistical distributions obtained for the $\{\beta_g\}$, $\{p_g\}$ and $\{\lambda_g\}$ for H_1 cycles highlight a natural division of the analysed networks in two broad classes (Fig. 2):

Class I networks: cycle distributions are markedly different from the randomized versions (cycles display shorter persistence times, earlier and broader birth distributions and very short lengths as compared to their randomized versions);

Class II networks: cycle distributions are very close to their random versions (late appearance, short persistences, long cycles).

The short cycles of Class I networks nest hierarchically and appear and die over all scales while those in the randomized counterparts are born uniformly along the filtration but are more persistent, producing largely hollow network instances. The implications are twofold. Since cycles represent weaker connectivity regions, this results in class I networks being more *solid* than the randomized versions, while class II networks resemble more closely the randomized instances. Second, since the cycle abundance ratio between real and random instances is the same in the two groups, the differences between class I and II does not depend on cycle abundance, but rather on their properties.

This can be seen easily by compressing the whole information within two scalar metrics which do not depend on the number of generators in a given network filtration. We define the *network hollowness* h_i and the *chain-length normalized hollowness* \tilde{h}_i as:

$$h_k = \frac{1}{N_{g_k}} \sum_{g_k} \frac{p_{g_k}}{T} \quad (2.1)$$

$$\tilde{h}_k = \frac{1}{N_{g_k}} \sum_{g_k} \frac{\lambda_{g_k}}{N} \frac{p_{g_k}}{T} \quad (2.2)$$

where $\{g_k\}$ is the set of generators of the k -th homological group H_k and $N_{g_k} = \dim H_k$ their number. The first is a measure of the average persistence, while the second weights generators according to both their length and persistence. Table 1 reports the values for h_1 and \tilde{h}_1 . Class I networks have lower hollowness values as compared to their randomized versions, while class II ones show comparable values. Interestingly, the hollowness values for the H_2 generators mostly vanish for the randomized instances (Table 1), as opposed to the case of real networks. It appears that, while persistent one-dimensional cycles are more easily generated in the randomized instances, higher forms of network coordinations, e.g. H_2 generators (akin to two-dimensional surfaces bounding three-dimensional voids), do not only display different properties in comparison to the real network, but are instead wiped away. These findings hint therefore to the presence of higher order coordination mechanisms in real world networks.

Naturally, the two network classes do not represent a binary taxonomy and should be considered as two extremes of a range over which networks distribute. For example, we find networks that interpolate between these classes, e.g. the online messages network has short persistence intervals, but also late cycle appearances and short length cycles. However, classes do not appear to display uniform behavior for local and two-body quantities: degree- and weight- distributions and correlations are mixed within the same group and do not provide a direct answer for the nature of the two classes. Similarly, a recently proposed measure of structural organisation, *integrativeness* [23], which measures the neighborhood overlap around strong links, does not provide insights to explain class I, since within the latter one finds both integrative and dispersive networks.

Finally, the classes do not show a consistent pattern in *assortativity*: for example, class I includes the gene network (assortative) and the airport networks (disassortative), while class II includes the assortative co-authorship networks and the disassortative Twitter data. Therefore, assortativity cannot be the discriminating factor between classes.

2.2 Higher order organization

Because homology is essentially a non-local property, it was expectable that the local measures just mentioned would not be able to explain the observed homological patterns. Network homology can be seen in fact as the weighted complement to the *perturbative dK-series* approach [8]: the latter proceeds by successive bottom-up constraints on k -body correlations, rapidly becoming very cumbersome, while

our method returns the complete superposition of the network’s degree and weight correlation layers in a non-perturbative (top-down) fashion.

A simple artificial network helps illustrating this point: Random Geometric Graphs (RGG) have been recently shown to display long-range many-body correlations [24, 25]. We find also that they have homological structures reminding of class I networks (Fig. 2a, b and c) and the same relation to their randomized versions. Class I networks are the result of high-order coordination in a similar way. This is supported also by the presence in real networks and RGGs of higher homology generators, which require elaborate coordination patterns in order to appear. While these cycles almost disappear in randomized versions of real-world networks, they are present in the case of RGGs.

For the latter and the airports, this organisation can be thought as the result of the non-local constraint imposed by the metric of the underlying space [26]. Although spatial constraints are harder to fathom for social and genetic systems, alternative explanations are possible: for example, the homological structure of the observed online communication and gene networks can be thought as stemming from group interactions among people (e.g. mailing lists, multi-user mails) and biological functions (e.g. pathways) respectively, which provide an underlying non-local mechanism for the emergence of homological patterns.

Further evidence of this behavior can be found by zooming on specific cycles which convey information about underlying constrains hidden in the network weight-link connectivity patterns. For example, the cycle structure of the air passenger network detects the expected reduced connectivity over oceans –in the form of strong persistent cycles– and the strong backbone of US airport hubs, which is then filled by the local (intra-community) links (Fig. 1b). Another example can be found in the school children’s face-to-face contact network. As expected we find the most significant cycles to link together different school classes (yellow and pink cycles in Fig. 1c). However, we also find that a school class (green nodes), despite being both a network community and 3-clique component [28], is characterized by a strong internal H_1 generator, which might be reflecting peculiar social dynamics coming from different seating arrangements or schedules for part of the class [29].

2.3 Spectral correlates of homology classes

At the opposite extreme of local quantities lie the spectral properties of networks. It is very important therefore to investigate whether it is possible to highlight peculiar spectral signatures of the two classes. Network eigenvalues, especially those of the Laplacian matrix, figure prominently in a number of applications, ranging from spectral clustering [30] to the propensity to synchronize of a set of oscillators distributed on the nodes [31]. Given a graph G , we denote its adjacency matrix $A(G)$ and its Laplacian matrix as $L(G) = D - A(G)$, where $d_{ij} = \delta_{ij} \sum_k a_{ik}$. For a symmetric network with N nodes, $A(G)$ has a set of real eigenvalues $\lambda_1 \geq \lambda_2 \geq \dots \lambda_{N-1} \geq \lambda_N$. The spectral gap $\Delta\lambda_A = \lambda_1 - \lambda_2$, and its normalized version, $R_A = \frac{\lambda_1 - \lambda_2}{\lambda_2 - \lambda_N}$, effectively measure how far the leading eigenvalue lies in comparison to the bulk of the eigenvalue distribution [32].

Interestingly, we find that class I networks have significantly larger spectral gaps ($p < 0.05$ comparing the distributions) than class II networks (panel IV in Fig. 2a). Despite being somewhat neglected in the complex networks literature, $\Delta\lambda_A$ has been linked to the notion of natural connectivity [33]: it encodes spectral information about network redundancy in terms of the number of closed paths and is defined as $\bar{\lambda} = \log \left[\frac{1}{N} \sum_{i=1}^N e^{\lambda_i} \right]$. Rewriting $\bar{\lambda} = \lambda_1 + \log \left[\frac{1}{N} (1 + \sum_{i=2}^N e^{\lambda_i - \lambda_1}) \right]$, it is easy to see that for large gaps all the terms in the sum are exponentially suppressed and therefore $\bar{\lambda}$ is essentially dominated by the leading adjacency eigenvalue modulo a size effect, $\bar{\lambda} \sim \lambda_1 - \log N$. This result is consistent with the nested cycle structure that we highlighted in class I. More importantly, we find a difference between the two classes in the topological constraints to synchronization processes . For the Laplacian $L(G)$, label the set of eigenvalues $0 = \lambda_1 < \lambda_2^L \leq \lambda_3^L \leq \dots \leq \lambda_N^L$ and define the Laplacian eigenratio $R_L = \frac{\lambda_N^L}{\lambda_2^L}$.

Barahona and Pecora [20] showed that a set of dynamical systems, placed on the network’s nodes and coupled according to the graph adjacency with a global coupling σ , has a linearly stable synchronous state if

$$R_L < \beta \tag{2.3}$$

where β is a purely dynamical parameter. This inequality implies that networks displaying very large R_L are hard (or impossible) to synchronize. Panel IVb of Fig. 2 shows again a significant difference between the two classes: class I networks have much larger eigenratios, making them hardly synchronizable.

Our results show therefore a deep connection between the homological network structure, the network spectral properties and their implications on network dynamics. Indeed, the role of mesoscopic structures in the stability and evolution of dynamical systems on networks is gradually emerging, as shown for example by recent work based on the concepts of basic symmetric subgraphs and their legacy eigenvalues in the global network spectrum [21], and is indeed being shaped by algebraic methods, well suited to capture the geometric information hidden within the network fabric.

3 Conclusions

Hitherto, the homological structure of weighted networks could not be systematically studied. Our method, grounded in computational topology, allows to probe multiple layers of organized structure. It highlighted two classes of network distinguished by their homological features, which we interpreted as caused by differences in the higher order networks organisations that are not captured by (quasi)local approaches.

Among the many possible applications, two very relevant ones for social and infrastructural networks are the study of the weighted rich club’s geometry beyond the aggregate measure [22, 34], and the generalisation of network embedding models to include homological information [35]. Furthermore, the two classes displayed also a marked difference in their spectral gap distributions and in particular in the values of the algebraic connectivity, implying that the different homological structures are correlated with different synchronizability thresholds.

This work therefore provides a stepping stone towards understanding the coupling between network dynamical processes and the network’s homology.

Finally, the filtration’s construction rule is flexible and can be readily adapted to other problems. Similarly to changing goggles, different edge metrics can be used (e.g. betweenness or salience [36]), the thresholding method varied (e.g. local thresholding [14]) or the filtration promoted to a filtering on two quantities (e.g. edge weight and time in a temporal network) using *multi-persistent* homology [37].

Methods and Materials

Persistent homology

The method we use to uncover weighted holes is persistent homology of the weight clique rank filtration. In this section we will briefly explain persistent homology and its realization through the weight rank clique filtration.

Persistent homology is a technique from computational algebraic topology that can be viewed as parametrized version of simplicial homology[38]. The two definitions needed for simplicial homology are those of *simplicial complex* and *homology*. A *simplicial complex* is a non empty family X of finite subsets, called faces, of a vertex set with the two constraints:

- a subset of a face in X is a face in X ,

- the intersection of any two faces in X is either a face of both or empty.

We assume that the vertex set is finite and totally ordered. A face of $n + 1$ vertices is called n -face and denoted by $[p_0, \dots, p_n]$. The interpretation of low dimensional faces is intuitive: a 0-face is a vertex, a 1-face is a segment, a 2-face is a full triangle, a 3-face is a full tetrahedron. The dimension of a simplicial complex is the highest dimension of the faces in the complex.

Morphism between simplicial complexes are called simplicial maps. A simplicial map is a map between simplicial complexes with the property that the image of a vertex is a vertex and the image of a n -face is face of dimension $\leq n$.

Simplicial Homology with coefficients in a field is a functor from the category of simplicial complexes to the category of vector spaces [38]. Homology of dimension n assigns to each simplicial complex X , the vector space $H_n(X)$ of n -cycles modulo boundaries and to every simplicial map $X \xrightarrow{f} Y$ the linear map $H_n(f) : H_n(X) \rightarrow H_n(Y)$.

The construction that leads to the vector space H_n is the following. Given a simplicial complex X of dimension d , consider the vector spaces C_n on the set of n -faces in X for $0 \leq n \leq d$. Elements in C_n are called n -chains. The linear maps sending a n -face to the alternate sum of its $(n - 1)$ -faces.

$$\begin{aligned} \partial_n : C_n &\longrightarrow C_{n-1} \\ [p_0, \dots, p_n] &\longrightarrow \sum_{i=0}^n (-1)^i [p_0, \dots, p_{i-1}, p_{i+1}, \dots, p_n]. \end{aligned}$$

shares the property $\partial_{n-1} \circ \partial_n = 0$.

The subspace $\ker \partial_n$ of C_n is called the vector space of n -cycles and denoted by Z_n . The subspace $\text{Im } \partial_{n+1}$ of C_n , is called the vector space of n -boundaries and denoted by B_n . Note that from $\partial_{n-1} \circ \partial_n = 0$ it follows that $B_n \subseteq Z_n$ for all n .

The n -th simplicial homology group of X , with coefficients in k , is the vector space $H_n := Z_n/B_n$.

Persistent homology is the homology of a *filtration*, i.e. an increasing sequence of simplicial complexes

$$X_0 \subset X_1 \subset \dots \subset X_n = X,$$

as opposed to that of a single simplicial complex.

It assigns to a filtration the homology groups of the simplicial complexes $H_n(X_v)$ and the linear maps $i_{v,w} : H_n(X_v) \rightarrow H_n(X_w)$ induced in homology by the inclusions $X_v \hookrightarrow X_w$ for all $v \leq w$. Note that the linear maps $i_{v,v+1}$ are not always injective, meaning that some homological features can disappear along the filtration. These features are encoded by the persistent homology generators: an element $g \in H_n(X_v)$ such that there is no $h \in H_n(X_w)$ for $w < v$ with the property that $i_{w,v-w}h = g$. Two indices completely determine a generator $g \in H_n(X)$, namely its birth, β_g and its death δ_g . The index β_g traces the first index such that g is in the filtration and δ_g is the index of the simplicial complex in which the cycle becomes a boundary (i.e. disappears homologically). The persistence (lifetime) of a generator is measured by $p_g := \delta_g - \beta_g$. The length of a cycle, that is the number of faces composing it, is denoted by λ_g .

For each homology group, the information about the filtration is collected in a barcode: the set of intervals $[\beta_g; \delta_g]$ for all generators $g \in H_n$, which constitutes a handy complete invariant of H_n [16]. An alternative way to represent the persistent homology of a filtration is through persistence diagrams [16, 39], which we use extensively in the SI. A persistence diagram is a set of points in the plane counted with multiplicity. It can be recovered from the barcode considering the points $(\beta_g, \delta_g) \in \mathbb{R}^2$ with multiplicity given by the number of generators with the same persistence interval. In the SI, the reader can find H_1 persistent diagrams of the real world datasets examined for the classification, together with the explicit comparison to the results for their relevant randomized versions.

Filtrations

In classical applications, the filtration is obtained from a point cloud using the Rips-Vietoris complex and persistent homology used to uncover robust topological features of the point cloud. We instead use the clique weight rank filtration to uncover properties deriving from the topology and weighted structure of weighted networks.

Recalling that an n -clique is a complete subgraph on $n + 1$ vertices, the *clique complex* is a simplicial complex built from the cliques of a graph. Namely there is a n -face in the simplicial complex for every $(n + 1)$ -clique in the graph. The compatibility relations are satisfied because subsets of cliques and intersection of cliques are cliques themselves.

The *Weight Rank Clique filtration* on a weighted network Ω combines the clique complex construction with a thresholding on weights following three main steps.

- Rank the weights of links from ω_{max} to ω_{min} : the discrete parameter ϵ_t indexes the sequence.
- At each step t of the decreasing edge ranking we consider the thresholded graph $G(\omega_{ij}, \epsilon_t)$, i.e. the subgraph of Ω with links of weight larger than ϵ_t .
- For each graph $G(\omega_{ij}, \epsilon_t)$ we build the clique complex $K(G, \epsilon_t)$.

The clique complexes are nested along the growth of t and determine the weight rank clique filtration. Note that this construction is in fact the clique complex of each element in the graph filtration.

In particular, persistent one dimensional cycles in the weight rank clique filtration represent weighted loops with much weaker internal links.

There is a conceptual difference in interpreting H_1 persistent homology of data with the Rips-Vietoris filtration and H_1 persistent homology of weighted networks with the weight rank clique filtration. While in the first case persistent generators are relevant and considered features of the data, short cycles are more interesting for networks. This is because random networks, or randomisations of real networks, display one dimensional persistent generators at all scales, while short lived generators testify the presence of local organisation properties on different scales.

Acknowledgments

The authors acknowledge M. Rasetti for stimulating discussions.

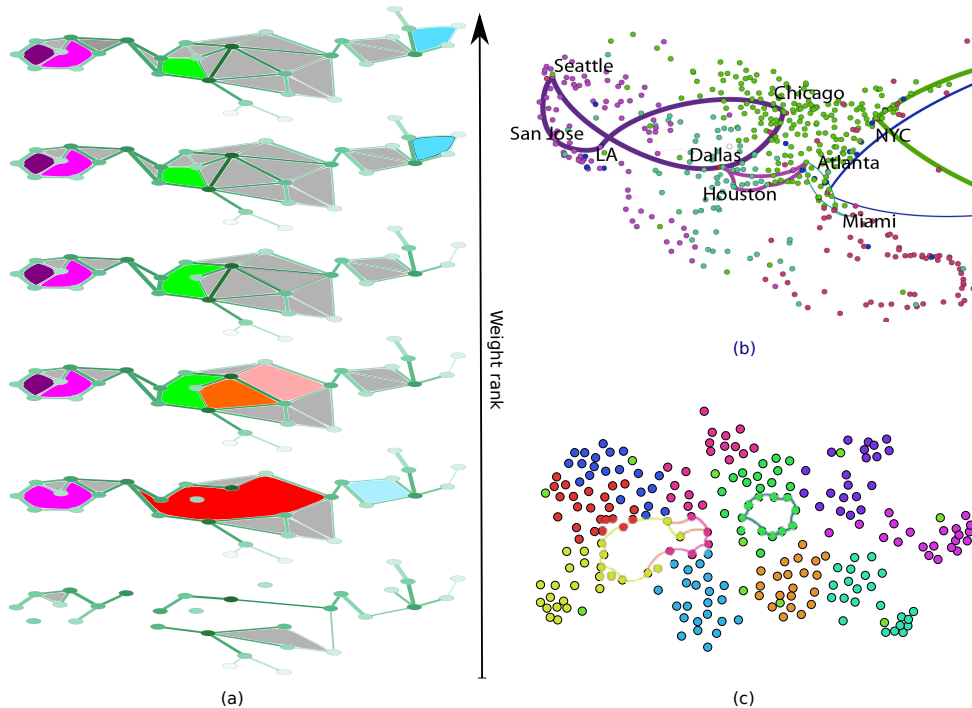


Figure 1. Weight rank clique filtration and homology of networks. (a) The weight rank filtration proceeds from the bottom up. Weighted holes (colored) and cliques (gray) appear as links are added. Weighted holes can branch into smaller holes, which have then independent evolution, persisting or dying along the filtration as links close them by 3-cliques. The cartoon shows two very long-persistence holes (violet and purple) appearing quite early and living until the end, while the largest hole (red) branches into three smaller holes, of only one survives to the end of the filtration (green). (b) A selection of weighted holes from the US air passenger network (year 2000). The node colors represent the best modularity partition of the entire network. The cycles are all long-persistence one, chosen to represent different behaviors: for example, the Chicago-Los Angeles-San Jose-Seattle cycle spans a large spatial distance, implying weaker connectivity across the cycle and within the region encompassed by the cycle, while the cycle going east from New York connects the east coast to three large European network and its persistence is due to the reduced connectivity due to the Atlantic Ocean. (c) A selection of the strongest cycles in the face-to-face contact network in a primary school (see SI for details on dataset). Node colors represent different classes in the school. Cycles are often found across communities, since by definition they probe the presence of holes among network regions. However, this is not the only information they convey. The cycle contained in a single community (green) testify the presence of peculiar contact geometries even within dense community structures.

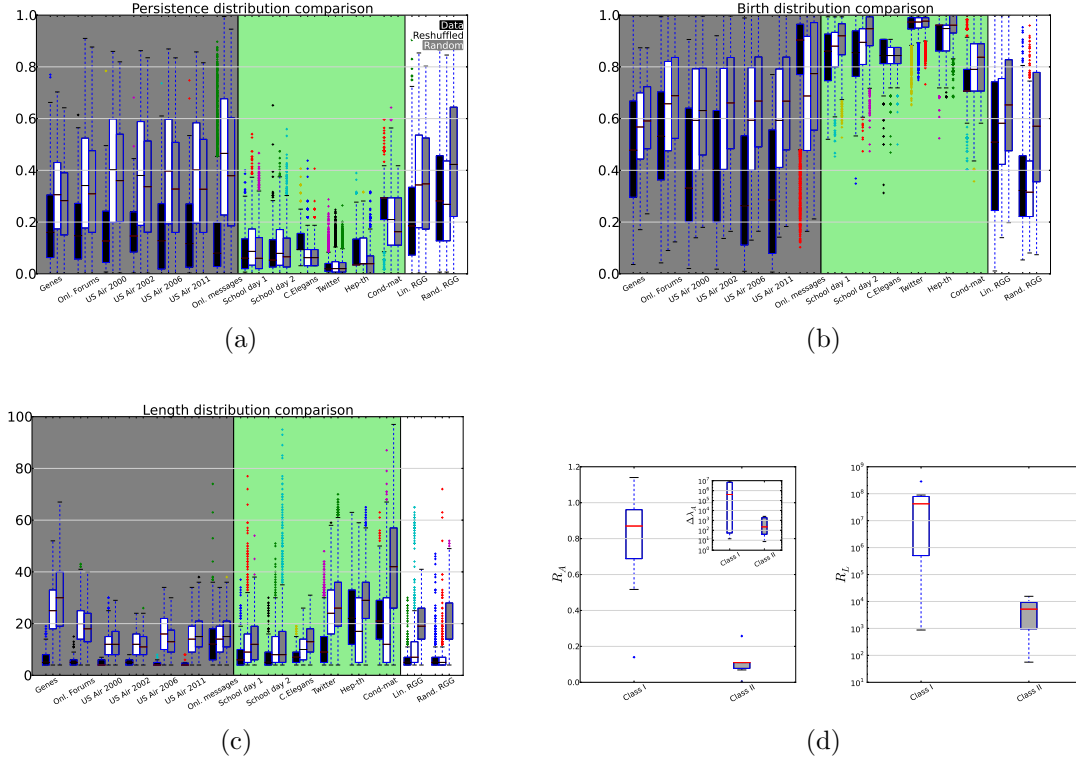


Figure 2. Figure 2. Statistical and spectral properties of H_1 generators. Box plots of the distributions of persistences $\{p_g\}$ (panel a)), births $\{\beta_g\}$ (panel b)) and lengths $\{\lambda_g\}$ (panel c)) for the 1d cycles (H_1 generators) of real networks (*black*), reshuffled (*white*) and randomized (*gray*). The gray and green shaded areas identify the two network classes described in the main text: class I is significantly different from the random expectations, with shorter, less persistent cycles that appear across the entire filtration; class II networks are not significantly different from the random versions, with long cycles and late birth times in the filtration. The characteristics of class I networks imply a stratification of cycles that betrays the presence of large, non-local organisation in the network structure, which is not present in class II networks. For comparison, an example of RGG network (600 nodes in the unitary disk, linking distance 0.01), known to have higher order degree correlations, had edge weights set according to $\omega_{ij} \propto (k_i k_j)^\theta$, with $\theta = 1$ (linearly correlated weight RGG) and $\theta = 0$ (random weight RGG). In both cases, the distributions of cycles' properties resemble closely those of class I networks. Panel d) finally reports the distribution of adjacency spectral gaps $\Delta\lambda_A$ and R_A (left plot) and the Laplacian eigenratio R_L (right plot). All the quantities show significant ($p < 0.05$) differences between the two classes, implying that the homological structure affect the dynamical properties of networks, e.g. the synchronizability threshold.

Dataset (class)	h_1	\tilde{h}_1	h_1^{sh}	\tilde{h}_1^{sh}	h_1^{rnd}	\tilde{h}_1^{rnd}	h_2	\tilde{h}_2
Genes(I)	0.515	0.003	0.020 ± 0.001	0.0007 ± 0.00001	0.0151 ± 0.0004	0.00023 ± 0.00005	0.35	0.006
Online forums(I)	0.175	0.001	0.355 ± 0.005	0.007 ± 0.001	0.325 ± 0.005	0.007 ± 0.001	0.02	0.0003
US Air 2000(I)	0.160	0.001	0.405 ± 0.005	0.0065 ± 0.0007	0.358 ± 0.006	0.0060 ± 0.0005	0.02	0.0003
US Air 2002(I)	0.186	0.0008	0.39 ± 0.01	0.0037 ± 0.0003	0.34 ± 0.01	0.0034 ± 0.0003	0.23	0.002
US Air 2006 (I)	0.167	0.0005	0.398 ± 0.005	0.0036 ± 0.0005	0.348 ± 0.008	0.0032 ± 0.0003	0.165	0.001
US Air 20011(I)	0.181	0.0006	0.41 ± 0.01	0.0034 ± 0.0002	0.35 ± 0.01	0.0033 ± 0.0003	0.076	0.0007
Online messages(I)	0.21	0.0014	0.190 ± 0.002	0.0017 ± 0.0001	0.185 ± 0.002	0.0015 ± 0.0001	0.02	0.0003
School day 1 (II)	0.088	0.0034	0.113 ± 0.002	0.007 ± 0.001	0.093 ± 0.002	0.006 ± 0.001	0.015	0.0012
School day 2 (II)	0.090	0.0033	0.115 ± 0.002	0.0065 ± 0.0005	0.098 ± 0.003	0.0089 ± 0.0008	0.01412	0.00095
C. elegans (II)	0.0784	0.002	0.0745 ± 0.0017	0.001 ± 0.0001	0.0896 ± 0.0023	0.0041 ± 0.0005	0.058	0.002
Twitter (II)	0.03	0.0001	0.030 ± 0.001	0.0002 ± 0.0001	0.029 ± 0.001	0.0002 ± 0.0001	0.01	0.0001
Hep-th (II)	0.08	0.0002	0.075 ± 0.001	0.0002 ± 0.0001	0.0508 ± 0.0003	0.0002 ± 0.0001	-	-
Cond-mat (II)	0.26	0.0004	0.20 ± 0.003	0.0002 ± 0.0001	0.180 ± 0.002	0.0005 ± 0.0001	-	-
Lin. RGG	0.227	0.003	0.368 ± 0.005	0.006 ± 0.001	0.355 ± 0.002	0.012 ± 0.001	0.28	0.006
Ran. RGG	0.3	0.0041	0.299 ± 0.005	0.0045 ± 0.0002	0.649 ± 0.40	0.015 ± 0.001	0.115	0.003

Table 1. Summary of hollowness values. For each dataset, we report the values of the *hollowness* h_1 and *cycle-length normalized hollowness* \tilde{h}_1 for H_1 cycles for real networks and their randomisations (*sh* and *rnd*). Most networks (class I in particular) show lower values than for their randomized versions. We also report the values of the *hollowness* h_2 and *cycle-length normalized hollowness* \tilde{h}_2 for H_2 cycles for real networks. The values for the randomized networks are not reported as –strikingly– the randomisations do not display any higher homology, while almost all real networks display positive values of the H_2 hollowness.

References

1. Newman M E J (2003), The Structure and Function of Complex Networks. *SIAM Rev.*, **45**(2), 167256.
2. Boccaletti S, Latora V, Moreno Y, Chavez M, and Hwang D H (2006), Complex networks: Structure and dynamics. *Phys. Rep.* **424**,(4-5), 175-308.
3. Dorogovtsev S N, Goltsev A V and Mendes J F F (2008), Critical phenomena in complex networks. *Rev. Mod. Phys.*, **80**(4), 1275–1335.
4. Barrat A, Barthlemy M, Pastor-Satorras R and Vespignani A (2004), The architecture of complex weighted networks. *Proc. Natl. Acad. Sci. USA* **101**, 3747–3752.
5. Barabási A (1999), Emergence of Scaling in Random Networks. *Science* **286**,509–512.
6. Milo R, Shen-Orr S, Itzkovitz S, Kashtan N, Chklovskii D and Alon U (2002), Network motifs: Simple building blocks of complex networks. *Science* **298** (5594): 824-827.
7. Vázquez A, Dobrin R, Sergi D, Eckmann J P, Oltvai Z N and Barabási A L (2004), The topological relationship between the large-scale attributes and local interaction patterns of complex networks. *Proc. Nat. Acad. Sci. USA*, **101**(52), 17940–17945.
8. Mahadevan P, Krioukov D, Fall K and Vahdat A (2006), Systematic topology analysis and generation using degree correlations. *ACM SIGCOMM*, **36**(4), 135146.
9. Conradi C, Flockerzi D, Raisch J and Stelling J (2007), Subnetwork analysis reveals dynamic features of complex (bio)chemical networks. *Proc. Natl. Acad. of Sci. USA*, **104**(49), 19175–19180.
10. Eguíluz V M, Chialvo D R , Cecchi G A , Baliki M and Apkarian A V (2005), Scale-Free Brain Functional Networks . *Phys. Rev. Lett.* **92**:028102.
11. Song W M, Di Matteo T and Aste T (2012), Hierarchical information clustering by means of topologically embedded graphs. *PloS One*, **7**(3), e31929.

12. Chalupa J, Leath P L, Reich G R (1979), Bootstrap percolation on a Bethe lattice. *J. Phys. C* **12**:L31.
13. Tumminello M, Aste T, Di Matteo T and Mantegna R. (2005), A tool for filtering information in complex systems. *Proc. Natl. Acad. Sci. USA*, **102**(30), 10421.
14. Serrano M, Boguñá M and Vespignani A (2009), Extracting the multiscale backbone of complex weighted networks. *Proc. Nat. Acad. Sci. USA*, **106**(16), 6483.
15. Ghrist R (2008), Barcodes: The persistent topology of data. *B. AM. Math. Soc.* **45**, 61.
16. Carlsson G and Zomorodian A (2005), Persistent homology-a survey. *Discrete Comput. Geom.* **33**(2), 249-274.
17. Carlsson G (2009), Topology and data. *Bulletin of the American Mathematical Society.* **46**(2), 255-308.
18. Evans T S (2010), Clique graphs and overlapping communities. *J. Stat. Mech.* **2010**, P12037.
19. Horak D, Maletić S and Rajković M 2009 Persistent homology of complex networks. *J. Stat. Mech.* **2009**,P03034
20. Barahona M and Pecora L M (2002), Synchronization in small-world systems. *Phys. Rev. Lett.*, **(89)** 5,054101.
21. MacArthur B D and Sánchez-García R J (2009), Spectral characteristics of network redundancy. *Phys. Rev. E*, **80**(2), 026117.
22. Opsahl T, Colizza V, Panzarasa P and Ramasco J J, (2008) , Prominence and Control: The Weighted Rich-Club Effect. *Phys. Rev. Lett.*, **101** (168702).
23. Pajevic S and Plenz D (2012), The organization of strong links in complex networks. *Nat. Phys.* **8**, 429–436.
24. Barthelemy M (2011), Spatial Networks. *Phys. Rep.* **499**:1–101.
25. Antonioni A, and Tomassini M (2012), Degree correlations in random geometric graphs. *Phys. Rev. E*, **86**(3), 037101.
26. Barrat A, Barthelemy M and Vespignani A (2005), The effects of spatial constraints on the evolution of weighted complex networks. *J. Stat. Mech.*, 2005(05), P05003.
27. Schaub, M. T., Delvenne, J.-C., Yaliraki, S. N., & Barahona, M. Markov Dynamics as a Zooming Lens for Multiscale Community Detection: Non Clique-Like Communities and the Field-of-View Limit. *PLoS One*, **7**(2), e32210, (2012)
28. Palla G, Derényi I, Farkas I & Vicsek T (2005), The effects of spatial constraints on the evolution of weighted complex networks. *Nature* **435**, 814–818.
29. Stehlé J et al. (2011), High-Resolution Measurements of Face-to-Face Contact Patterns in a Primary School. *PLoS One* **6**(8): e23176.
30. Gfeller D and De Los Rios P (2007) , Spectral coarse graining of complex networks. *Phys. Rev. Lett.*, **99**(3), 38701.
31. Chavez M, Hwang D U, Amann A, Hentschel H G E and Boccaletti S (2005), Synchronization is Enhanced in Weighted Complex Networks. *Phys. Rev. Lett.*, **94**(21), 218701.

32. Farkas I J, Derenyi I, Barabási A L and Vicsek T (2001), Spectra of “real-world” graphs: Beyond the semicircle law. *Phys. Rev. E*, **64**(2), 026704.
33. Jun W U, Barahona M, Yue-Jin T and Hong-Zhong D (2010), Natural connectivity of complex networks. *Chin. Phys. Lett.*, **27**(7), 078902.
34. Colizza V, Flammini A, Serrano M A and Vespignani A (2006), Detecting rich-club ordering in complex networks. *Phys.* **2**(2), 110–115.
35. Boguñá M, Papadopoulos F and Krioukov, D. (2010), Sustaining the Internet with hyperbolic mapping. *Nat. Comms.*, **1**(6), 1–8.
36. Grady D, Thiemann C and Brockmann D (2012), Robust classification of salient links in complex networks. *Nat. Comm.*, **3**, 864.
37. Carlsson G and Zomorodian A (2009) Theory of multidimensional persistence. *Discr. Comput. Geom.*, **42**(1), 71-93.
38. Munkres, J R, (1984), Elements of Algebraic Topology *Addison-Wesley Publishing Company, Inc.*, 2725 Sand Hill Road Menlo Park, California 94025.
39. Steiner D C, Edelsbrunner H and Harer J (2007), Stability of persistence diagrams. *Discrete Comput. Geom.* **37**(1), 103-120.

Supplementary Information for "Topological strata of weighted complex networks"

The Supplementary Information is organized in four sections. Section I contains definitions and references concerning persistent homology, our main tool. In section II some constructions for filtrations are presented, in particular the weight rank clique filtration is introduced. In section III we describe the datasets tested for our main result, the classification of networks based on persistent H_1 generators. In section IV the reader can find more details on the classification, and the plots supporting the result.

Persistent homology

This section is devoted to the mathematical framework supporting persistent homology [1] [2] [3]. Persistent homology can be viewed as parametrized version of simplicial homology, that requires the definitions of simplicial complex and homology, for detailed information we refer to [4].

Definition 3.1. *A simplicial complex is a non empty family X of finite subsets, called faces, of a vertex set with the two constraints:*

- a subset of a face in X is a face in X ,
- the intersection of any two faces in X is a face of both.

We assume that the vertex set is finite and totally ordered. A face of $n + 1$ vertices is called n -face and denoted by $[p_0, \dots, p_n]$. A 0-face is a vertex, a 1-face is a segment, a 2-face is a full triangle, a 3-face is a full tetrahedron. The dimension of a simplicial complex is the highest dimension of the faces in the complex.

Example 3.2. *The clique complex is a simplicial complex constructed from a graph. There is a n -face in the simplicial complex for every $(n + 1)$ -clique in the graph, i.e a complete subgraph on $n + 1$ vertices. The compatibility relations are satisfied because subsets of cliques and intersection of cliques are cliques themselves.*

Morphism between simplicial complexes are called simplicial maps.

Definition 3.3. *A simplicial map is a map between simplicial complexes with the property that the image of a vertex is a vertex and the image of a n -face is face of dimension $\leq n$.*

Fixed a field k , in the following by vector space we intend a k -vector space and $k[t]$ is the polynomial ring in one variable with coefficients in k . Given a simplicial complex X of dimension d , consider the vector spaces C_n on the set of n -faces in X for $0 \leq n \leq d$. Elements in C_n are called n -chains. The linear maps sending a n -face to the alternate sum of it's $(n - 1)$ -faces.

$$\begin{aligned} \partial_n : C_n &\longrightarrow C_{n-1} \\ [p_0, \dots, p_n] &\longrightarrow \sum_{i=0}^n (-1)^i [p_0, \dots, p_{i-1}, p_{i+1}, \dots, p_n]. \end{aligned}$$

shares the property $\partial_{n-1} \circ \partial_n = 0$.

The subspace $\ker \partial_n$ of C_n is called the vector space of n -cycles and denoted by Z_n . The subspace $\text{Im } \partial_{n+1}$ of C_n , is called the vector space of n -boundaries and denoted by B_n . Note that from $\partial_{n-1} \circ \partial_n = 0$ it follows that $B_n \subseteq Z_n$ for all n .

Definition 3.4. The n -th simplicial homology group of X , with coefficients in k , is the vector space $H_n := Z_n/B_n$. The rank of H_n is called the n -th Betti number of X .

The first Betti numbers of X have an easy intuitive meaning: the 0-th Betti number is the number of connected components of X , the first Betti number is the number of two dimensional (polygonal) holes, the third Betti number is the number of three dimensional holes (convex polyhedron).

It is fundamental to note that homology is a functor, this implies the following proposition.

Proposition 3.5. Let X and Y be two simplicial complexes, a simplicial map $f : X \rightarrow Y$ determines a linear map between the homology groups $H_i(f) : H_i(X) \rightarrow H_i(Y)$ for all i .

The starting point in persistent homology is a filtration. As in [2], we call a simplicial complex X filtered if we are given a family of subspaces $\{X_v\}$ parametrized by \mathbb{N} , such that $X_v \subseteq X_w$ whenever $v \leq w$. The family $\{X_v\}$ is called a *filtration*. There are many ways to construct a filtration from a point cloud or a network, some relevant ones are explained in section II.

Definition 3.6. The persistent homology module of a filtration is given by the homology groups of the simplicial complexes $H_n(X_v)$ and the linear maps $i_{v,w} : H_n(X_v) \rightarrow H_n(X_w)$ induced in homology by the inclusions $X_v \hookrightarrow X_w$ for all $v \leq w$.

Following [2], this system is called a module because the vector space $H_n = \bigoplus_v H_n(X_v)$ can actually be endowed with a $k[t]$ -module structure, defining $t \cdot m := i_{v,v+1}(m)$ for $m \in H_n(X_v)$. Note that the linear maps $i_{v,v+1}$ are not always injective. A persistent homology generator is a generator of H_n according to the $k[t]$ -structure, i.e an element $g \in H_n(X_v)$ such that there is no $h \in H_n(X_w)$ for $w < v$ with the property that $t^{v-w}h = g$. By the structure theorem on modules over PID, $k[t]$ -modules are completely determined by the degree of each generator g (birth of the generator β_g) and the degree in which the generator is annihilated by the module action (death of the generator δ_g). The persistence (lifetime) of a generator is measured by $p_g := \delta_g - \beta_g$. The length of a cycle, number of faces composing it, is denoted by λ_g .

The barcode of a filtration is the set of intervals $[\beta_g; \delta_g]$ for all generators $g \in H_n$, this is a handy complete invariant of H_n , [2]. By persistent topological features we intend generators of H_n such that the interval $[\beta_g; \delta_g]$ is large with respect to the filtration length.

An alternative way to represent persistent homology modules is the persistence diagram [3], [5]. A persistence diagram is a set of points in the plane counted with multiplicity, it can be recovered from the barcode considering the points $(\beta_g, \delta_g) \in \mathbb{R}^2$ with multiplicity given by the number of generators with the same persistence interval.

Persistent homology modules can be computed using the libraries *javaPlex* (Java) or *Dionysus* (C++), which are both available from the Stanford's CompTop group website (<http://comptop.stanford.edu/>), and presented using the barcode or the persistence diagram. We developed a Python module to wrap the *javaPlex* library, consisting of a number of scripts able to preprocess complex networks and store the resulting homological information in a manageable form.

Filtrations

In this section we will go through some basic constructions that generate a filtration starting from a point cloud or a complex network.

The most popular filtration for data analysis is the *Rips-Vietoris filtration* [2]. The Rips-Vietoris complex is a simplicial complex associated to a set of points in a metric space in the following way: every point p is the center of a radius ϵ ball $D(p, \epsilon)$ and $n + 1$ points $\{p_0, \dots, p_n\}$ determine a n -face in the

Rips-Vietoris complex if the corresponding radius ϵ balls intersect two by two, i.e. $D(p_i, \epsilon) \cap D(p_j, \epsilon) \neq \emptyset$ for all $i \neq j \in \{0 \dots n\}$. Clearly the Rips-Vietoris complex depends on the parameter ϵ and if $\epsilon_1 < \epsilon_2$ the complex with ϵ_1 radius balls is contained in the complex with ϵ_2 radius balls. To the growth of ϵ we obtain an increasing sequence of simplicial complexes, a filtration, the Rips-Vietoris filtration. In this context persistent topological features of the filtration are considered as features of the point cloud.

For unweighted networks, the *Clique filtration* is used in [6] to analyse the difference between the barcodes of random networks, networks with exponential connectivity distribution and scale-free networks. The k -skeleton X_k of a simplicial complex X is the subcomplex of X containing all the faces of dimension smaller or equal to k . Consider a complex network and the corresponding clique complex X , the clique filtration is obtained by filtering the clique complex according to the dimension of the skeleton:

$$X_0 \subseteq X_1 \subseteq X_2 \subseteq \dots \subseteq X.$$

Note that persistent features of the Clique filtration are generators of the homology groups of the clique complex. These generators can be directly calculated from the clique complex of the graph, thus the filtration gives no extra information. This is not the case for the following filtration we have introduced for weighted networks in which persistent features cannot be determined from a single simplicial complex in the family but instead reveal the intricate multiscale relation between weights and links in a weighted indirect network.

The *Weight Rank Clique filtration* on a weighted network Ω combines the clique complex construction with a thresholding on weights. The first step is to rank the weights of links from ω_{max} to ω_{min} : the discrete parameter ϵ_t scans the sequence. At each step t of the decreasing edge ranking we consider the thresholded graph $G(\omega_{ij}, \epsilon_t)$, i.e. the subgraph of Ω with links of weight larger than ϵ_t . For each graph $G(\omega_{ij}, \epsilon_t)$ we build the clique complex $K(G, \epsilon_t)$. The clique complexes are nested to the growth of t and determine the weight rank clique filtration. Persistent one dimensional cycles represent weighted loops with much weaker internal links.

Datasets

The dataset analysed in this paper cover a broad range of fields, spanning social, infrastructural and biological networks. In detail they are:

US Air passenger networks The networks refer to the years 2000, 2002, 2006 and 2011. The years were chosen to provide snapshots of the air traffic situation at 4-5 years intervals, plus one extra (year 2000) just before the events of 9/11 which significantly affected the air transportation industry. The data used are publicly available from the website of the Bureau of Transportation Statistics (<http://www.transtats.bts.gov/>). Individual flights between airports were aggregated on routes as defined by origin and destination cities. The weight reported is the yearly aggregated passenger traffic.

C. Elegans The network is available at <http://cdg.columbia.edu/cdg/datasets> and reports a weighted, directed representation of the C. Elegans's neuronal network [7]. The network was symmetrized by summing the weights present on edges between the same nodes (given ω_{ij} and ω_{ji} , $\omega_{ij}^{symm} = \omega_{ji}^{symm} = \omega_{ij} + \omega_{ji}$).

Online Messages and Forums The online messages network consists of messages in a student online community at University of California [8]. The online forum network refers to the same online community, but focuses on the activity of users in public forums, rather than on private messages [9]. Both networks are publicly available online at Tore Opsahl's website (<http://toreopsahl.com/datasets/>).

Gene network The gene interaction network used in the paper is a sampling of the complete human genome dataset available from the University of Florida Sparse Matrix Collection. Each node is an individual gene, while the edges correlates the expression level of a gene with that of the genes (using a NIR score [10]). The node set of the analysed network was obtained by randomly choosing an origin node, then adding its neighborhood to the node set; the neighborhoods of the newly added nodes were then added to the node set recursively until a given number of nodes was obtained (in the case used the target number of nodes was $N = 1300$). Then all the edges present in the original network between the nodes in the node set were added, effectively taking a connected subgraph of the original network. To reduce the computational complexity due to the large density of the graph, the weighted clique filtration was stopped at an edge weight of 0.09 (similarly to the choice made in [11]).

Twitter The dataset consists of a network of mentions and retweet between Twitter users and is available online on the Gephi dataset page (<http://wiki.gephi.org/index.php/Datasets>). Weights are proportional to the number of interactions between a pair of users.

School face-to-face contact network The dataset contains two days of recorded face-to-face interactions in a primary school. Each node represents a child, with the edge weight between two nodes being proportional to the amount of time the two children spent face to face. We analysed the two days separately, yielding two networks. The dataset has been collected by the Sociopattern project (<http://www.sociopatterns.org/>) and analysed in [12].

Co-authorship networks The networks analysed are the weighted co-authorship networks of the Condensed Matter E-print Archive between 1995 and 1999 (cond-mat) and the High-Energy Theory E-print Archive between 1995 and 1999 (hep-th) [13].

Finally, for comparison we use Random Geometric Graphs (RGG) [14, 15], which are simple models of spatial networks: a RGG is generated by sprinkling N of nodes randomly on a metric space that acts as a substrate (usually a disk of unitary radius or a square with identified edges), and then linking nodes that are closer than a given linking distance d .

Finally, the networks analysed in this article are undirected and weighted, because the weighted clique filtration finds a natural application in such case. However, schemes for directed networks can be easily devised and tailored to specific case studies, e.g. one could adopt the definition used in the directed clique percolation method [16] in order to associate network structures to simplices.

Results for weight rank clique filtration

We recall that given a network G on N nodes, we consider the weight clique rank filtration on G . Let T be the length of the filtration, $\{g_i\}$ the set of generators of the i -th persistence homology module of the filtration and N_{g_i} the cardinality of $\{g_i\}$. For every generator g_i , the index p_{g_i} is its persistence interval, the index λ_{g_i} is its length and β_{g_i} is its birth index. For brevity, H_1 generators will be denoted by g rather than g_1 .

There is a conceptual difference in interpreting H_1 persistent homology of data with the Rips-Vietoris filtration and H_1 persistent homology of weighted networks with the weight rank clique filtration. While in the first case persistent generators are relevant and considered features of the data, short cycles are more interesting for networks. This is because random networks, or randomisations of real networks, display one dimensional persistent generators at all scales, while short lived generators testify the presence of local organisation properties on different scales.

As stated in the main text, the complex networks we considered fall in two main groups.

Networks in group I display clear departures from the null counterparts, while class II networks show

homological features that are much closer to the randomized versions. We collected the complete information about the indices p_g , λ_g and β_g for persistent H_1 generators within a series of tableaux (Figures S.3 to S.17). In every figure, panel *a*) represents the distribution of persistence p_g , panel *b*) the distribution of length λ_g and panel *c*) the distribution of birth index β_g . These quantities are studied for the homology generators in the real world network (red circles), after weight reshuffling of the network (blue squares) and in the network randomisation (green triangles). Panel *d*) is the persistence diagram of the network under study, panel *e*) is the persistence diagram of its weight reshuffled null model and panel *f*) is the persistence diagram of the random null model.

From the perspective of persistence diagrams, class I presents a rich structure of nested cycles covering all scales, as opposed to the weight reshuffled null model and random null model where generators are born uniformly along the filtration and tend to be very persistent, producing largely hollow network instances. The degree and weight sequences are preserved in the randomisations and therefore cannot account for the differences in the homology. Another possibility to explain the different behavior of the two classes could be the presence of degree-degree or weight-degree correlations in class I. However, networks in the two classes do not show consistent patterns of assortativity: for example, class I includes the gene network (assortative) and the airport networks (disassortative), while class II includes the assortative co-authorship networks and the disassortative Twitter data. Also weight-degree correlations do not appear to be decisive: for example, the RGGs generated with random edge weights did not show significant differences from those generated with edge weights correlated positively to the degrees of the end nodes (see Figs. S.16 and S.17).

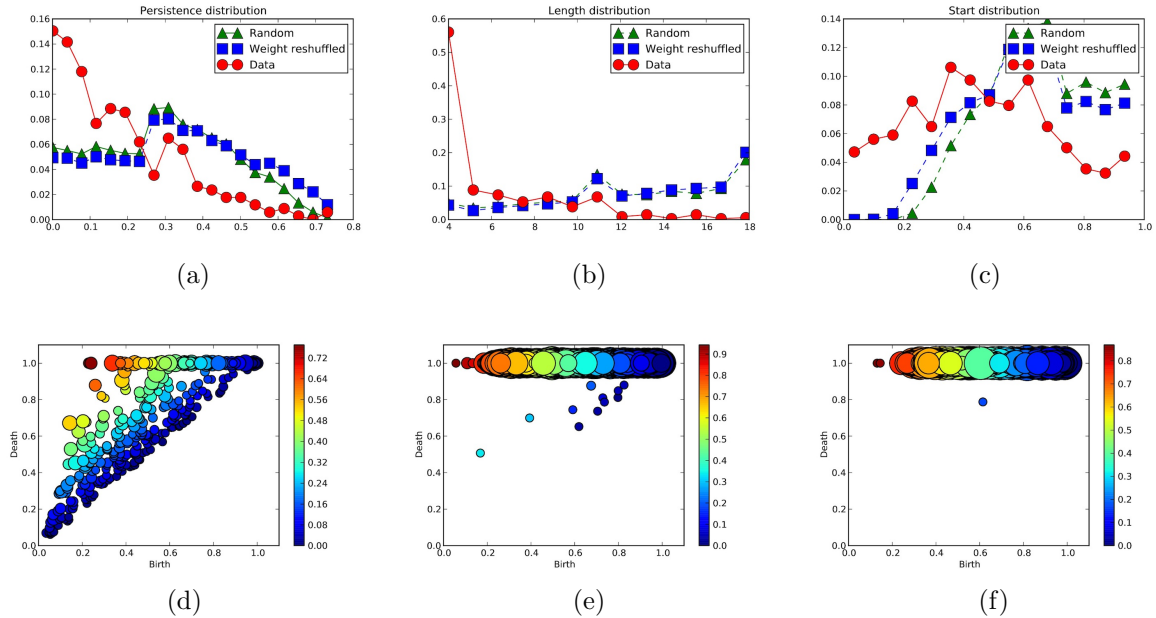


Figure S.3. Summary of H_1 persistent homology results for the human gene interaction network 2 (Class I).

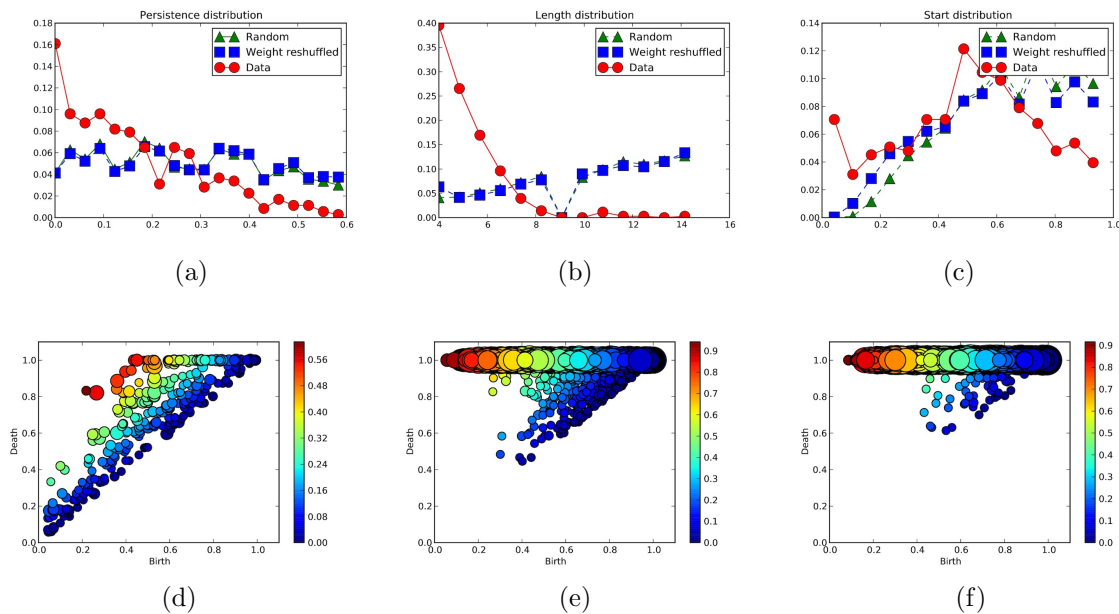


Figure S.4. Summary of H_1 persistent homology results for online forum network of [9] (Class I).

References

1. Carlsson, G., Topology and Data. *Bulletin of the American Mathematical Society*. **46(2)**, 255-308 (2009).
2. Carlsson,G. & Zomorodian,A., Computing Persistent Homology. *Discrete Comput. Geom.* **33(2)**, 249-274 (2005).
3. Edelsbrunner,H. & Harer, J., Persistent homology - a survey. *Cont. Math.*, 257-282, (2008).
4. Munkres, J.R., Elements of Algebraic Topology *Addison-Wesley Publishing Company, Inc.*, 2725 Sand Hill Road Menlo Park, California 94025 (1984).
5. Steiner,D.C. & Edelsbrunner, H. & Harer, J. Stability of Persistence Diagrams. *Discrete Comput. Geom.* **37(1)**, 103-120 (2007).
6. Horak D, Maletić S and Rajković M 2009 Persistent homology of complex networks. *J. Stat. Mech.* **2009**,P03034
7. Watts, D. J. & Strogatz, S. H. Collective dynamics of 'small-world' networks. *Nature* **393**, 440-442 (1998)
8. Opsahl, T. & Panzarasa, P., Clustering in weighted networks. *Soc. Net.* **31**, (2), 155-163, (2009)
9. Opsahl, T., Triadic closure in two-mode networks: Redefining the global and local clustering coefficients. *Soc. Net.*, (2010), 10.1016/j.socnet.2011.07.001
10. Gardner,T.S., di Bernardo,D., Lorenz,D., & Collins,J.J., Inferring genetic networks and identifying compound mode of action via expression profiling. *Science* **301**, 102-105 (2003).

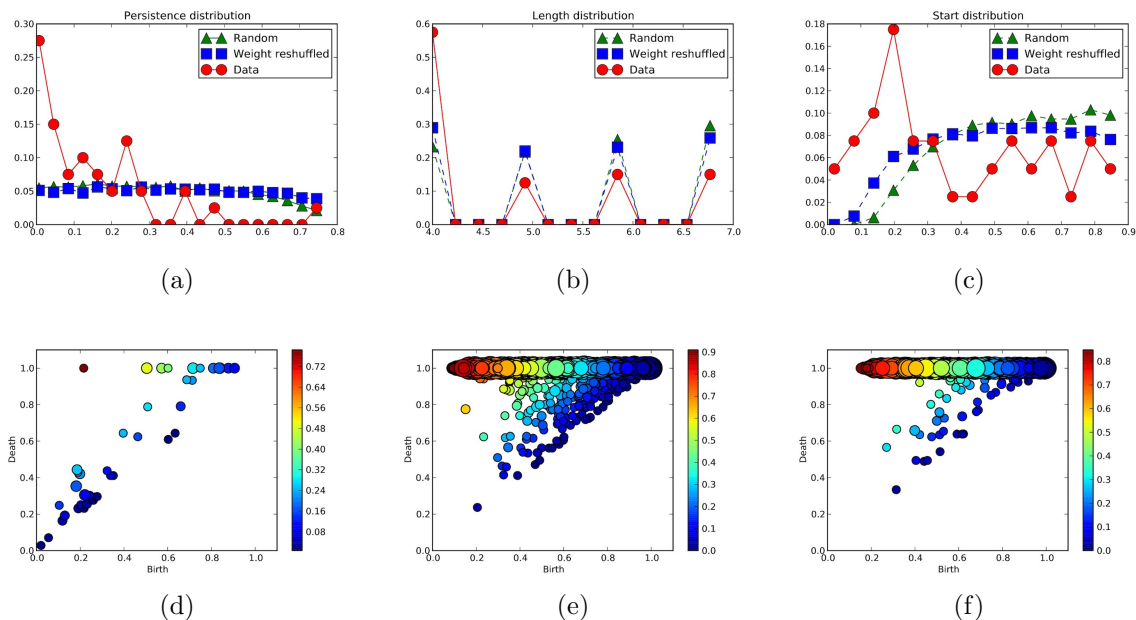


Figure S.5. Summary of H_1 persistent homology results for the US airways passenger network for 2000 (Class I).

11. Pajevic, S. & Plenz, D., The organization of strong links in complex networks. *Nat. Phys.*, **8**, 429-436 (2012).
12. Stehlé, J. et al., High-Resolution Measurements of Face-to-Face Contact Patterns in a Primary School. *PLoS One* **6**(8): e23176 (2011)
13. Newman, M. E. J. The structure of scientific collaboration networks, *Proc. Natl. Acad. Sci. USA* **98**, 404-409 (2001).
14. Barthélemy, M., Spatial Networks *Phys. Rep.* **499**, 1 (2011).
15. Penrose, M., Random Geometric Graphs *Oxford University Press*, Oxford, UK, (2003).
16. Palla, G. et al. Directed network modules. *New J. Phys.* **9**, (2007)

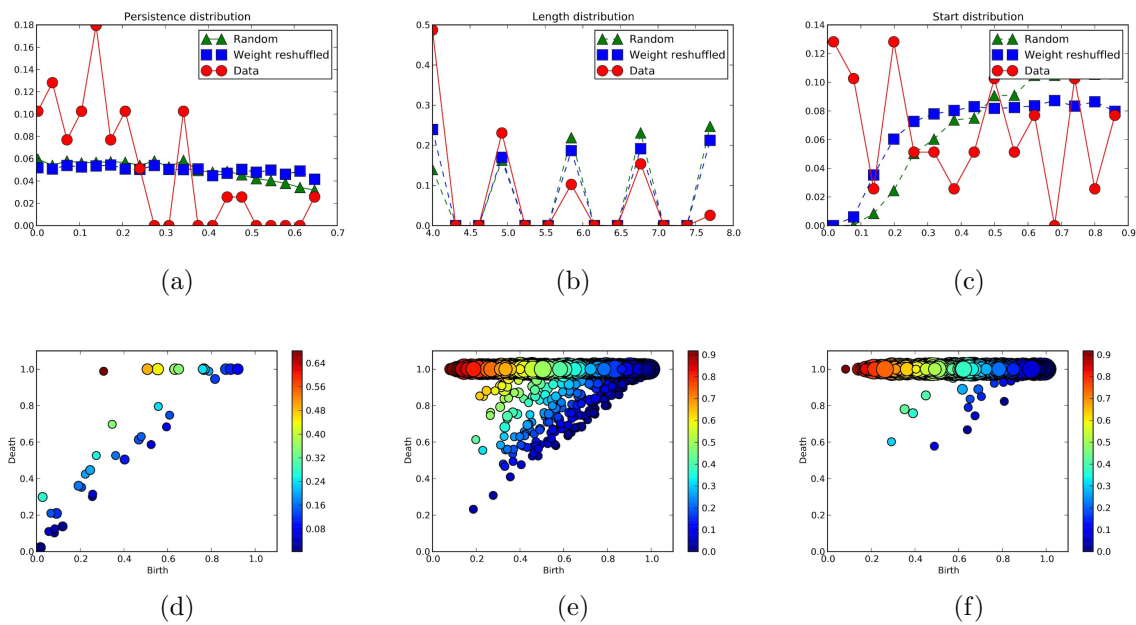


Figure S.6. Summary of H_1 persistent homology results for the US airways passenger network for 2002 (Class I).

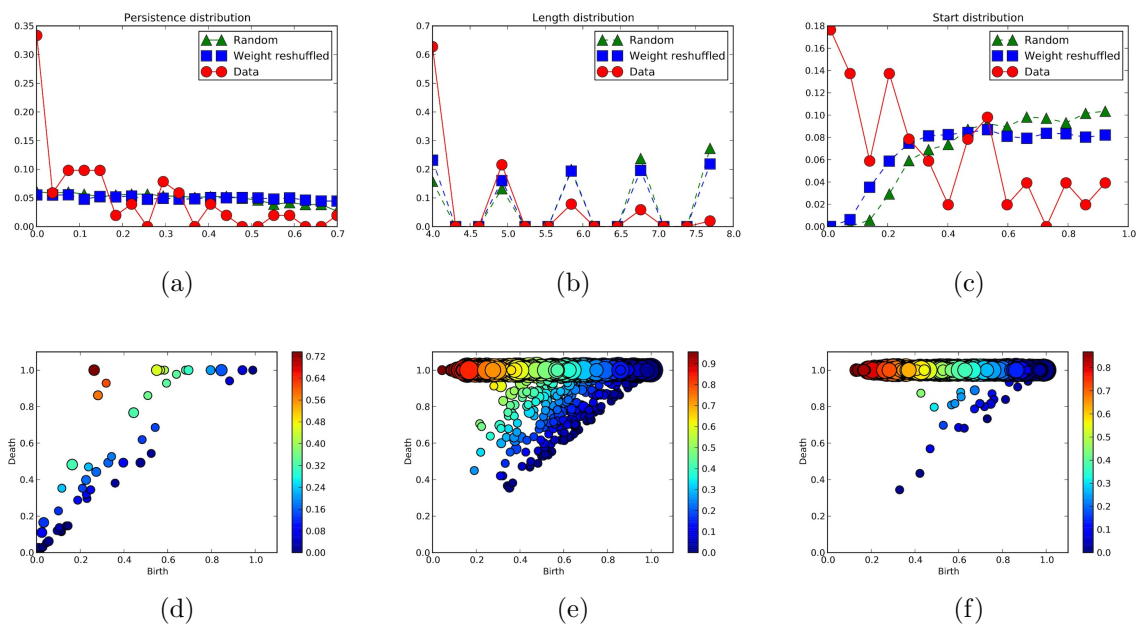


Figure S.7. Summary of H_1 persistent homology results for the US airways passenger network for 2006 (Class I).

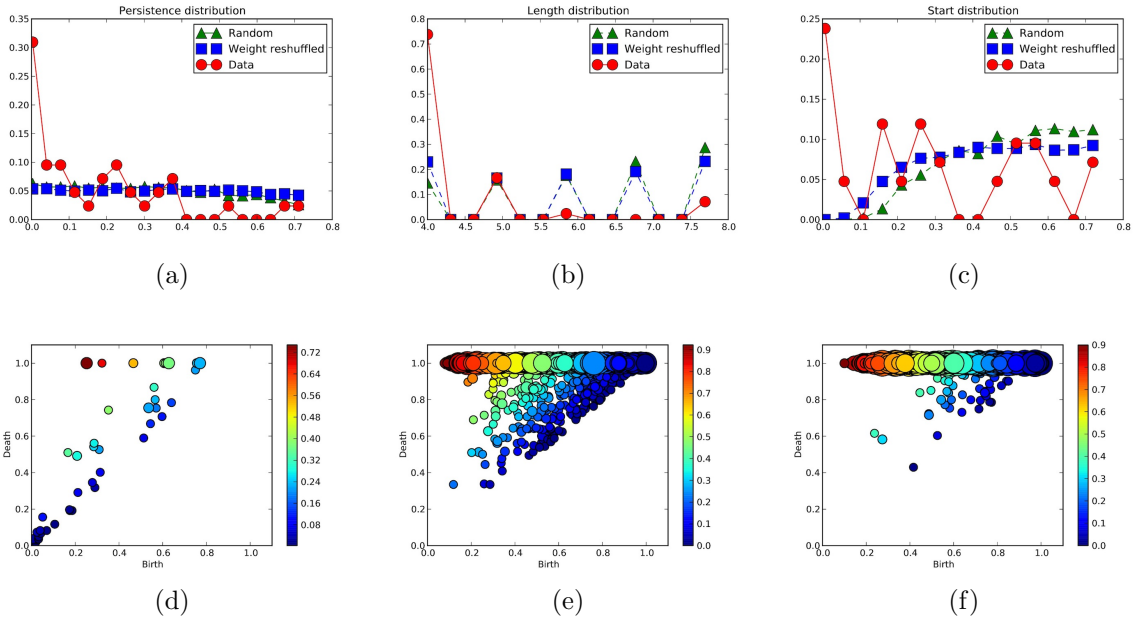


Figure S.8. Summary of H_1 persistent homology results for the US airways passenger network for 2011(Class I).

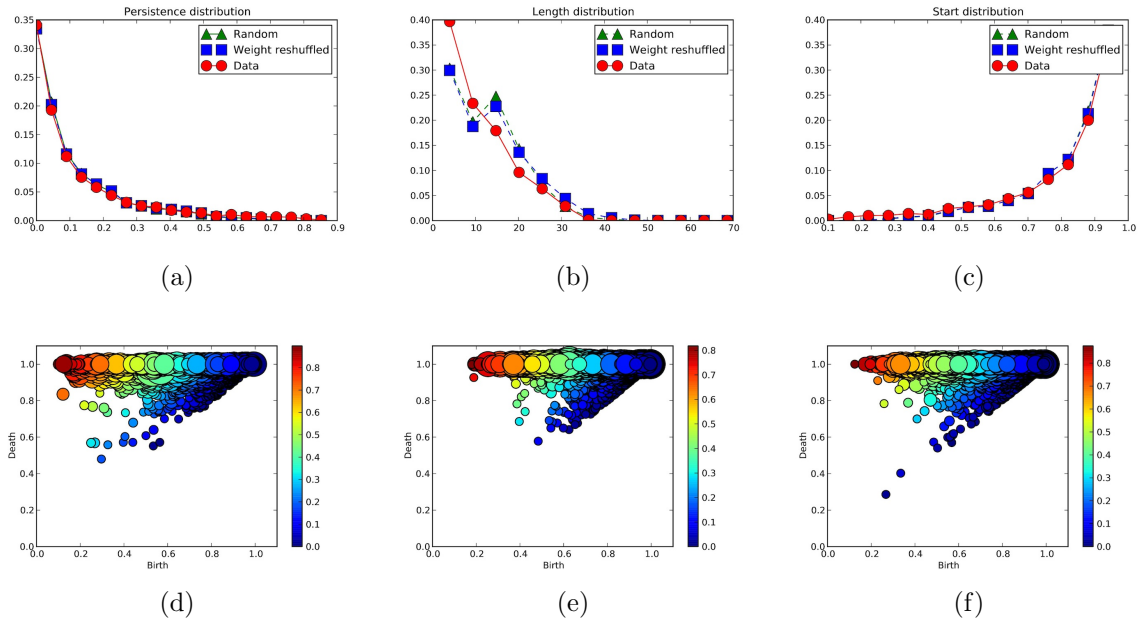


Figure S.9. Summary of H_1 persistent homology results for the online messages network of [8] (Class I).

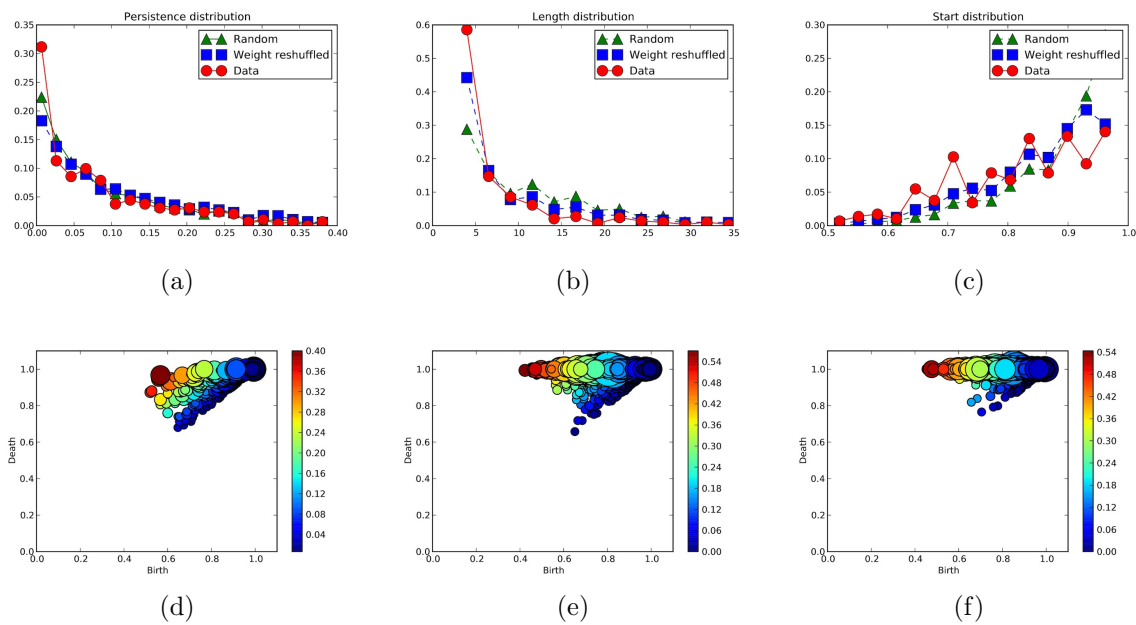


Figure S.10. Summary of H_1 persistent homology results for the day 1 face-to-face contact duration network of children of [12] (Class II).

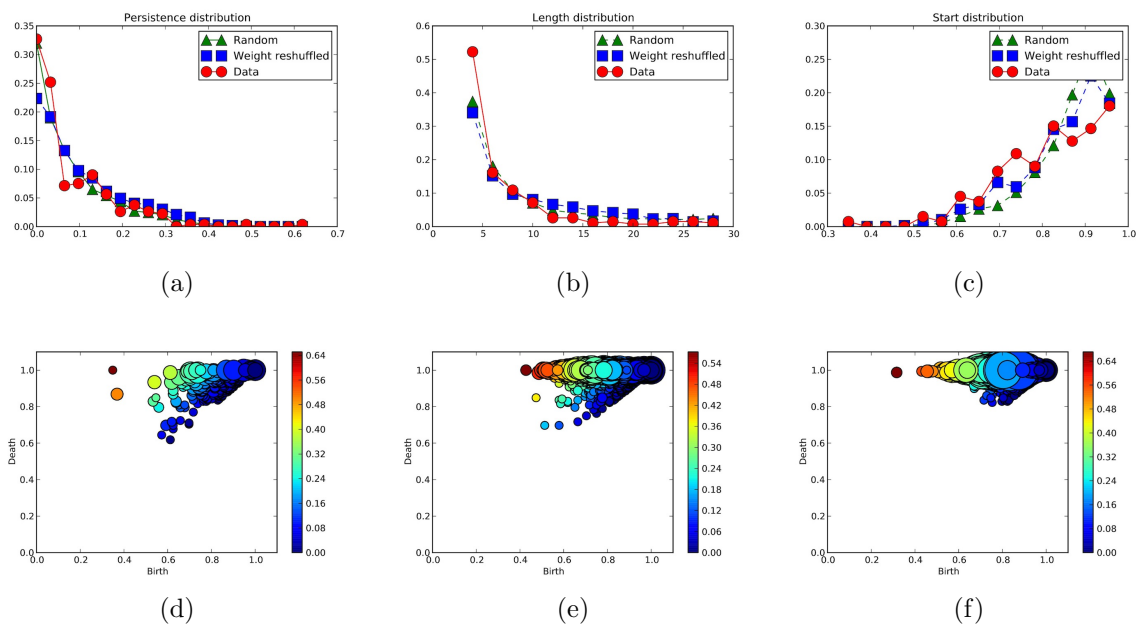


Figure S.11. Summary of H_1 persistent homology results for the day 2 face-to-face contact duration network of children of [12] (Class II)

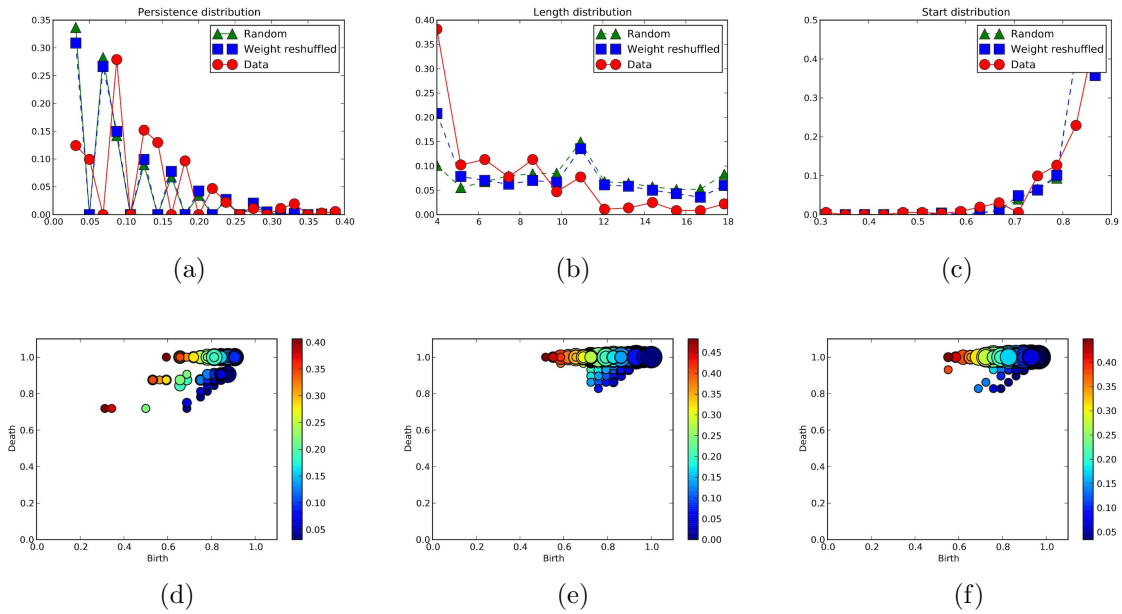


Figure S.12. Summary of H_1 persistent homology results for the neural network of the *C. elegans* (Class II).

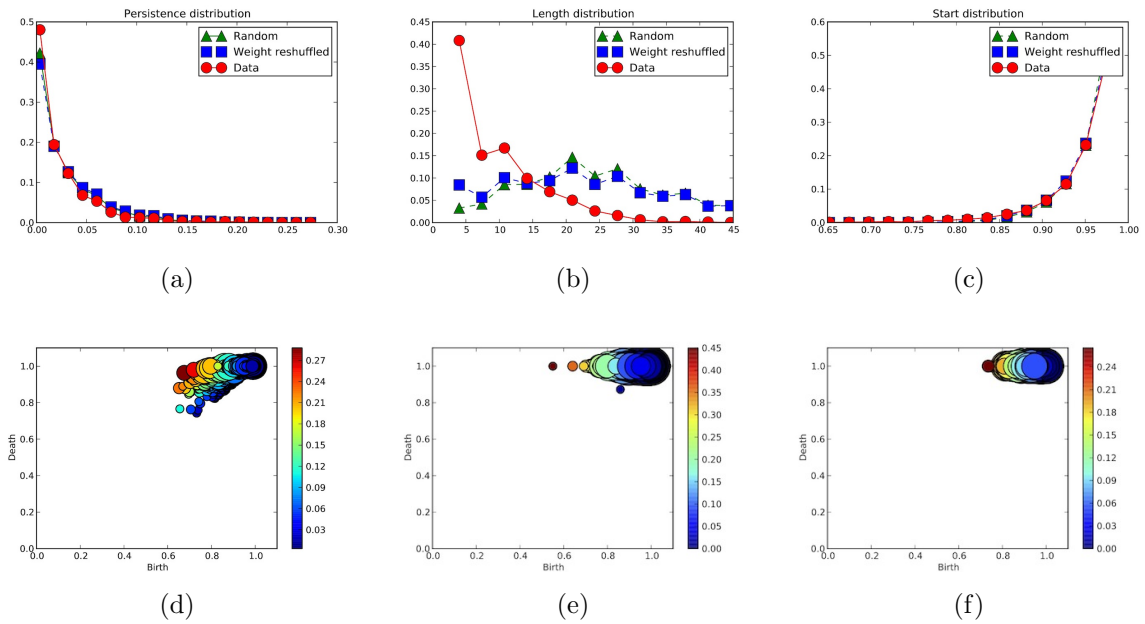


Figure S.13. Summary of H_1 persistent homology results for a network of mentions and retweets of a part of the Twitter network (Class II).

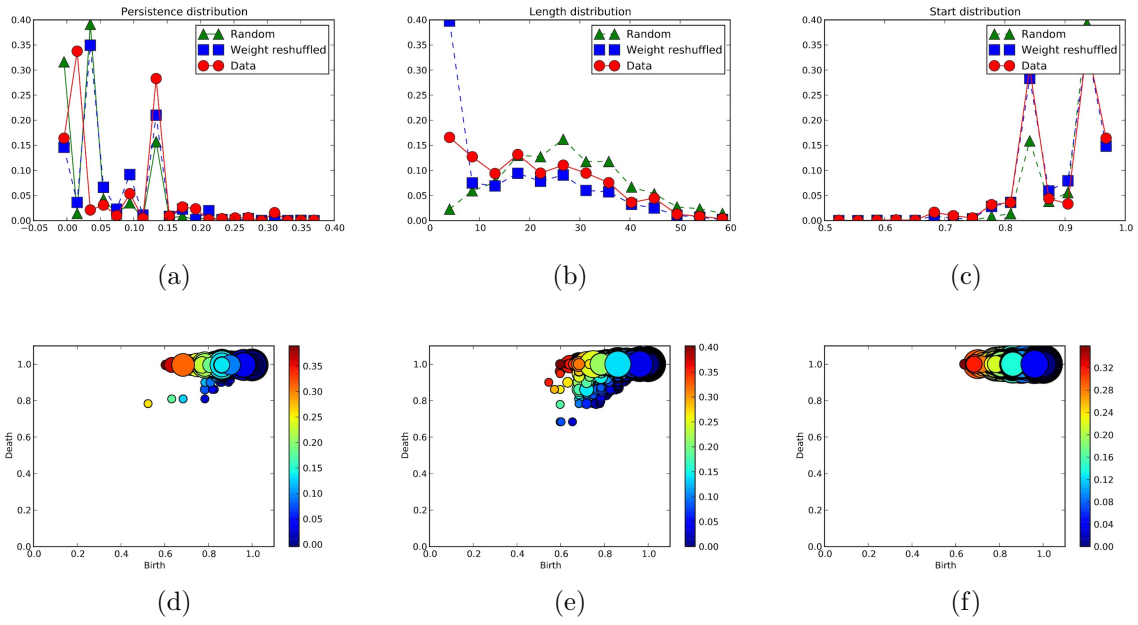


Figure S.14. Summary of H_1 persistent homology results for the Hep-th arxiv....(Class II)

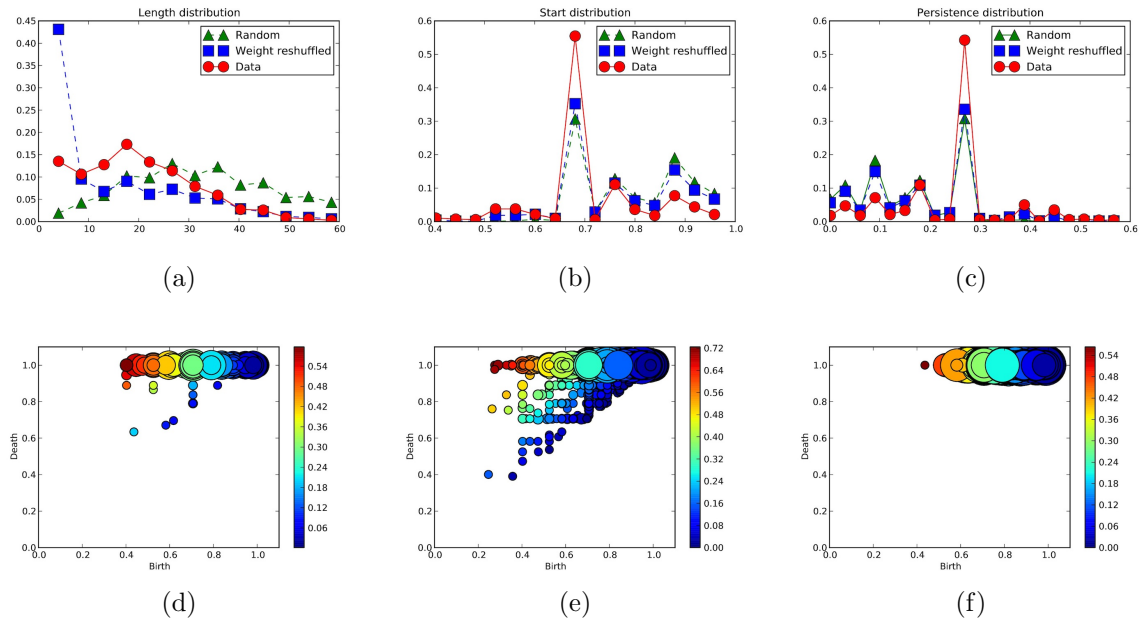


Figure S.15. Summary of H_1 persistent homology results for the cond-mat (Class II).

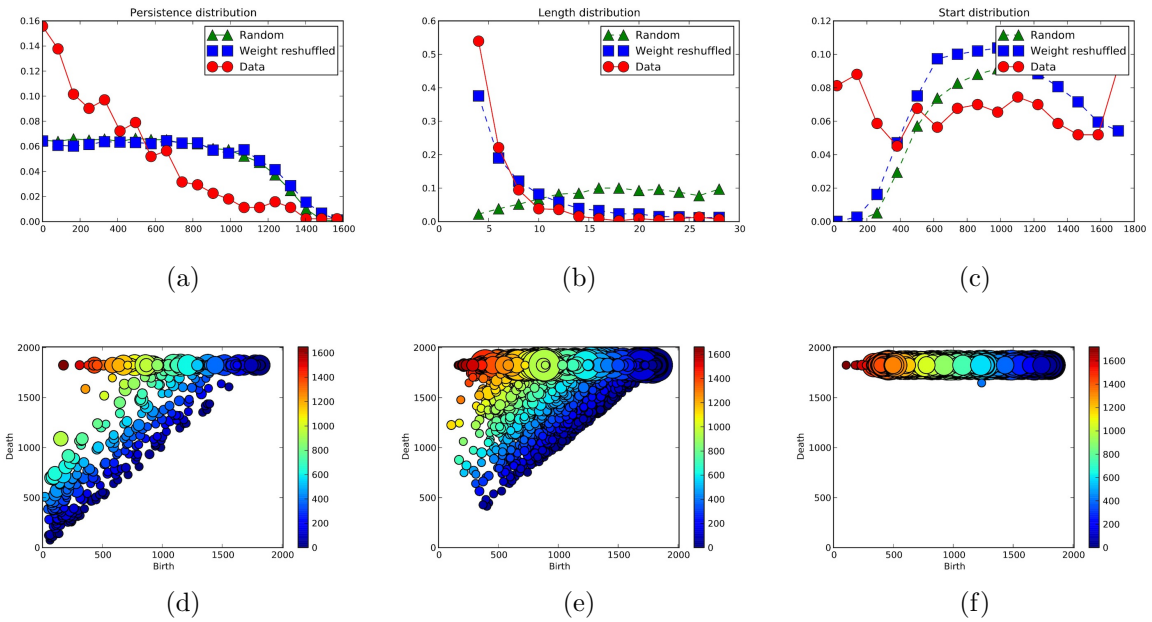


Figure S.16. Summary of H_1 persistent homology results for the Random Geometric Graph model with linear weight-degree correlations (Class I). The graph has $N = 600$ nodes and a linking distance $d = 0.01$. The weight of a link between nodes i and j was set according to $\omega_{ij} \sim (k_i k_j)^\theta X$, where $\theta = 1$ and X is a uniform random variable in $(0, 1)$.

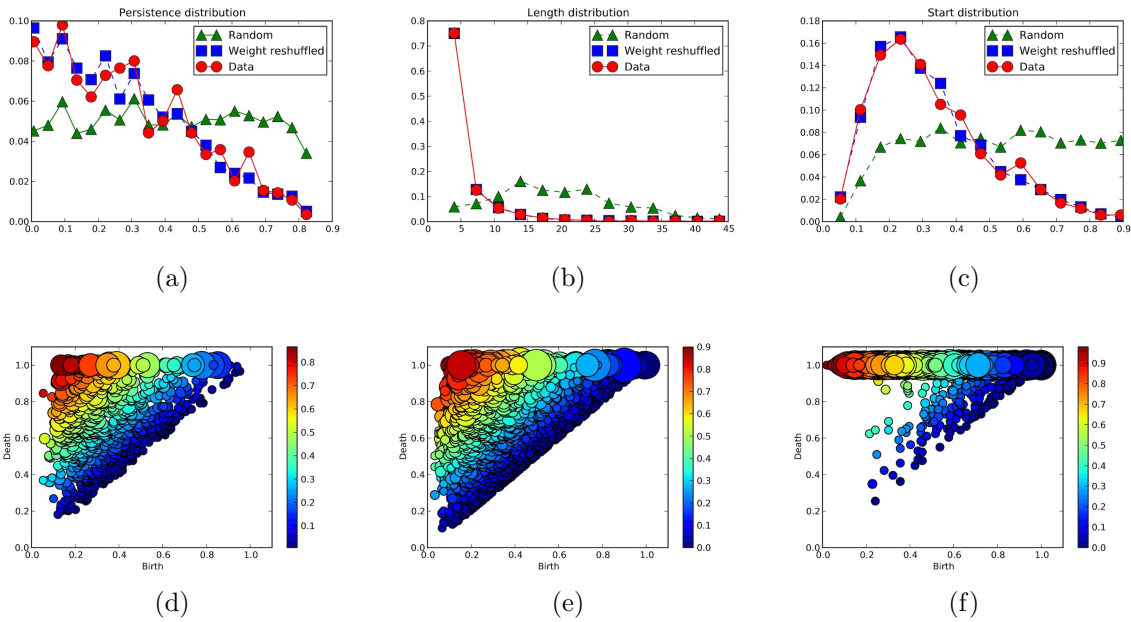


Figure S.17. Summary of H_1 persistent homology results for the Random Geometric Graph model with linear weight-degree correlations (Class I). The graph has $N = 600$ nodes and a linking distance $d = 0.01$. The weight of a link between nodes i and j was set with random uniform weights .